

Effect of laser-frequency fluctuation on the decay rate of Rydberg coherenceBongjune Kim,¹ Ko-Tang Chen,¹ Chia-Yu Hsu,¹ Shih-Si Hsiao,¹ Yu-Chih Tseng,¹ Chin-Yuan Lee,¹ Shih-Lun Liang,¹ Yi-Hua Lai,¹ Julius Ruseckas,² Gediminas Juzeliūnas,² and Ite A. Yu^{1,3,*}¹*Department of Physics, National Tsing Hua University, Hsinchu 30013, Taiwan*²*Institute of Theoretical Physics and Astronomy, Vilnius University, Saulėtekio 3, 10257 Vilnius, Lithuania*³*Center for Quantum Technology, Hsinchu 30013, Taiwan*

(Received 20 February 2019; published 9 July 2019)

The effect of electromagnetically induced transparency (EIT) combined with Rydberg-state atoms provides high optical nonlinearity to efficiently mediate the photon-photon interaction. However, the decay rate of Rydberg coherence, i.e., the decoherence rate, plays an important role in optical nonlinear efficiency and can be largely influenced by laser frequency fluctuation. In this work, we carried out a systematic study of the effect of laser frequency fluctuation on the decoherence rate. We derive an analytical formula that quantitatively describes the relationship between the decoherence rate and laser frequency fluctuation. The formula is experimentally verified by using the Λ -type EIT system of laser-cooled ^{87}Rb atoms, in which one can either completely eliminate or controllably introduce the effect of laser frequency fluctuation. We also include the effect of Doppler shift caused by the atomic thermal motion in the formula, which can be negligible in the Λ -type EIT experiment but significant in the Rydberg-EIT experiment. Utilizing the atoms of $350\ \mu\text{K}$, we study the decoherence rate in the Rydberg-EIT system involving the state of $|32D_{5/2}\rangle$. The experimental data are consistent with the predictions from the formula. We are able to achieve a rather low decoherence rate of $2\pi \times 48\ \text{kHz}$ at a moderate coupling Rabi frequency of $2\pi \times 4.3\ \text{MHz}$.

DOI: [10.1103/PhysRevA.100.013815](https://doi.org/10.1103/PhysRevA.100.013815)**I. INTRODUCTION**

Utilizing the strong dipole-dipole interaction (DDI) between Rydberg-state atoms in the applications of quantum information processing, such as realization of quantum logic gates [1–3], generation of single photons [4,5], and quantum simulations [6,7], is of great interest currently. These applications are made possible by the DDI-induced blockade effect, the phenomenon that multiple excitations to a Rydberg state within the blockade radius is strongly suppressed [8–17]. On the other hand, the effect of electromagnetically induced transparency (EIT) provides high optical nonlinearity [18–20]. Hence, the EIT effect combined with Rydberg-state atoms can efficiently mediate the photon-photon interaction, offering a powerful tool for quantum information manipulation with photons [21–28]. Furthermore, the storage of light based on the EIT effect can prolong the atom-photon or photon-photon interaction time [29–36]. Assisted by long lifetimes of Rydberg states, all-optical switching or a cross-phase shift with single photons and single-photon subtraction have been demonstrated with the light-storage scheme in the Rydberg-EIT system [34–36].

Similar to the Raman or ground-state coherence being the coherence between the two ground states in the Λ -type EIT (abbreviated as Λ -EIT) system depicted in Fig. 1(a) [37,38], the Rydberg coherence is the coherence between the ground and Rydberg states in the Rydberg-EIT system depicted in Fig. 1(b). The decay rate of Rydberg coherence,

i.e., the decoherence rate, can greatly influence the optical nonlinear efficiency of the Rydberg-EIT effect [39–43]. Because laser frequency fluctuation increases the decoherence rate, it also deteriorates the nonlinear efficiency. Hence, laser frequency fluctuation can be a problem in the high-fidelity low-loss quantum processes utilizing the Rydberg-EIT scheme.

The Λ -EIT system in Fig. 1(a) is driven by the probe and coupling fields in the Λ -type configuration. The frequency difference between the probe and coupling lasers determines the two-photon detuning. One can employ the phase-lock or injection-lock scheme to completely eliminate the laser frequency fluctuation from this frequency difference. Thus, the EIT resonant condition is stabilized to a high degree [44] and the laser frequency fluctuation is not a problem in the Λ -EIT experiment. On the other hand, the Rydberg-EIT system in Fig. 1(b) is driven by the probe and coupling fields in the ladder-type configuration. The sum of the probe and coupling frequencies determines the two-photon detuning. The schemes of reference cavities, high-resolution wavemeters, EIT spectroscopy, etc., were employed for the stabilization of laser frequencies in the Rydberg-EIT experiments [45–47]. However, the laser frequency fluctuation resulting from any stabilization method still contributes to this frequency sum and makes the experimental condition deviate from the EIT resonance. Thus, the laser frequency fluctuation is an unavoidable problem in the Rydberg-EIT experiment.

In Refs. [48,49], Li and co-workers developed a theory for Doppler-broadened EIT media and also considered the effect of the laser linewidth. They experimentally studied the

*yu@phys.nthu.edu.tw

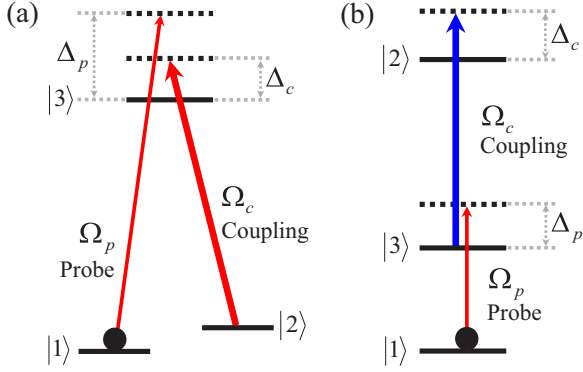


FIG. 1. Relevant energy levels and laser excitations in (a) the Λ -EIT system and (b) the Rydberg-EIT system. We employed laser-cooled ^{87}Rb atoms in the experiment. In (a), states $|1\rangle$ and $|2\rangle$ correspond to the ground states $|5S_{1/2}, F=1, m_F=1\rangle$ and $|5S_{1/2}, F=2, m_F=1\rangle$, and state $|3\rangle$ corresponds to the excited state $|5P_{3/2}, F=2, m_F=2\rangle$. In (b), states $|1\rangle$, $|2\rangle$, and $|3\rangle$ correspond to the ground state $|5S_{1/2}, F=2, m_F=2\rangle$, the Rydberg state $|32D_{5/2}, m_J=5/2\rangle$, and the excited state $|5P_{3/2}, F=3, m_F=3\rangle$, respectively.

theory in the ladder-type system with a room-temperature atomic vapor. In Ref. [50] Lü *et al.* experimentally investigated how the peak transmission of the Λ -EIT system is influenced by frequency fluctuation of the coupling field with a room-temperature atomic vapor. However, the effect of the frequency fluctuation was phenomenologically introduced in this reference. In Refs. [39,47] Weatherill and co-workers used a similar way to introduce the laser frequency fluctuation to the decoherence rate in their Rydberg-EIT experiments. Here we carry out a systematic study of the effect of laser frequency fluctuation on the decoherence rate. We derive a formula that quantitatively describes the relationship between the decoherence rate and laser frequency fluctuation and explicitly shows the roles of the coupling Rabi frequency and the optical depth in the relationship. The derived formula is experimentally verified in both the Λ -EIT and Rydberg-EIT systems with cold ^{87}Rb atoms.

This article is organized as the followings. In Sec. II we derive an analytical formula showing the decoherence rate as a function of the laser frequency fluctuation. Since the Doppler shift caused by the atomic thermal motion is not negligible in our Rydberg-EIT system, we also include the effect of the Doppler shift in the formula. In Sec. III we report the test result on the validity of the formula in the Λ -EIT system. Figure 3 illustrates the methods that determine the coupling Rabi frequency, optical depth, and decoherence rate. Figure 4 demonstrates that experimental data of the decoherence rate in the Λ -EIT system are consistent with predictions from the formula. In Sec. IV we report the study on the decoherence rate in the Rydberg-EIT system. The Rydberg state $|32D_{5/2}\rangle$ was selected in the study to avoid the DDI effect [51]. Figure 6 provides information about the atom temperature. The purpose of Fig. 7 is the same as that of Fig. 3. Figures 8 and 9 demonstrate that experimental data of the decoherence rate in the Rydberg-EIT system are consistent with predictions from the formula. Finally, we summarize in Sec. V.

II. THEORETICAL MODEL

Considering the two transition diagrams in Fig. 1, we derive an analytic formula that relates the decoherence rate of ρ_{21} to the laser frequency fluctuation. In Fig. 1(a), ρ_{21} is the coherence between the two ground states. In Fig. 1(b), ρ_{21} is the coherence between the ground state and the Rydberg state. The logic behind the derivation is the following. Although the laser frequencies are locked to the resonance frequency of the two-photon transition, their fluctuations randomly induce two-photon detunings to the EIT system. The two-photon detuning leads to attenuation or loss of the probe field. The average value of attenuations of various two-photon detunings caused by the laser frequency fluctuation can be seen as the result of an effective decoherence rate. A larger amplitude of the laser frequency fluctuation represents a greater root-mean-square value of the two-photon detuning, which causes more attenuation, similar to a larger decoherence rate. Therefore, the decoherence rate can be expressed as a function of the fluctuation amplitude.

We employ the optical Bloch equation (OBE) for the density-matrix operator of the atomic ensemble and the Maxwell-Schrödinger equation (MSE) for the probe field in the derivation, giving [52]

$$\frac{\partial}{\partial t} \rho_{21} = \frac{i}{2} \Omega_c \rho_{31} + i\delta \rho_{21} - \gamma_0 \rho_{21}, \quad (1)$$

$$\frac{\partial}{\partial t} \rho_{31} = \frac{i}{2} \Omega_p + \frac{i}{2} \Omega_c \rho_{21} + i\Delta_p \rho_{31} - \frac{\Gamma}{2} \rho_{31}, \quad (2)$$

$$\frac{1}{c} \frac{\partial}{\partial t} \Omega_p + \frac{\partial}{\partial z} \Omega_p = \frac{i\alpha\Gamma}{2L} \rho_{31}. \quad (3)$$

Here ρ_{21} and ρ_{31} are the density-matrix elements, Ω_p and Ω_c denote probe and coupling Rabi frequencies, γ_0 is the decoherence rate, Γ represents the spontaneous decay rate of the excited state $|3\rangle$, which is $2\pi \times 6.1$ MHz in our case, δ is the two-photon detuning of the Raman or Rydberg transition $|1\rangle \rightarrow |2\rangle$, Δ_p denotes the one-photon detuning of the probe transition $|1\rangle \rightarrow |3\rangle$, and α and L represent the optical depth (OD) and length of the medium, respectively.

To achieve the above OBE and MSE, we consider the weak probe field as a perturbation [52] and neglect the effect of dipole-dipole interaction among the Rydberg atoms. Only the slowly varying amplitudes of the density-matrix elements and those of the probe and coupling Rabi frequencies remain in the equations. All parts of the equations, except δ , are the same for both the Λ -EIT system shown in Fig. 1(a) and the Rydberg-EIT system shown in Fig. 1(b). The two-photon detuning is $\delta = \Delta_p - \Delta_c$ for the situation shown in Fig. 1(a) and $\delta = \Delta_p + \Delta_c$ for that in Fig. 1(b), where Δ_c is the one-photon detuning of the coupling transition.

To find the EIT spectral profile, we use Eqs. (1) and (2) and obtain the following steady-state solution for ρ_{31} :

$$\rho_{31} = \frac{\delta + i\gamma_0}{\Omega_c^2/2 - 2(\Delta_p + i\Gamma/2)(\delta + i\gamma_0)} \Omega_p. \quad (4)$$

The imaginary and real parts of ρ_{31} determine the output transmission and phase shift of the probe field, respectively. We are only interested in the transmission. Under the typical EIT condition of $\Omega_c^2 \gg 2\gamma_0\Gamma$ and $\Omega_c^2 \gg 4\delta\Delta_p$, the absorption

saturated-absorption spectroscopy. The time constant of the feedback loop in the frequency stabilization system was about 3 ms. Since the coupling and probe lasers were seeded or injection locked by the light beams from the ECDL, their frequency difference was fixed with a high degree of stability. An electro-optic modulator generated 6.8-GHz sidebands in the ECDL beam and the upper sideband locked the probe laser frequency. Acousto-optic modulators (AOMs) were used to switch the coupling field, generate Gaussian pulses of the probe field, and shift the frequencies of the two fields. As the probe and coupling fields interacted with the atoms, their e^{-2} diameters were 0.30 and 4.4 mm, respectively. We set the maximum Rabi frequency of the probe field to about 0.036Γ , which is weak enough to be treated as the perturbation in the theoretical model. A photomultiplier tube detected the probe light and its output voltage was recorded by an oscilloscope (Agilent MSO6014A). All the experimental data presented in the paper were averaged for 512 times by the oscilloscope.

The experimental parameters of coupling Rabi frequency Ω_c , optical depth α , and decoherence rate γ were determined in the way illustrated by the example in Fig. 3. First, we measured the separation distance between two transmission minima, i.e., the Autler-Townes splitting, to determine Ω_c as shown in Fig. 3(a). According to Eq. (4), the two minima occur at $\delta_{\pm} = (\Delta_c \pm \sqrt{\Delta_c^2 + \Omega_c^2})/2$, where Δ_c is the one-photon detuning of the coupling field. At $\Delta_c \ll \Omega_c$, $\delta_+ - \delta_- \approx \Omega_c + \Delta_c^2/2\Omega_c$. Since we carefully minimized Δ_c in the measurement, the correction term $\Delta_c^2/2\Omega_c$ was about $1.3 \times 10^{-4}\Gamma$ in Fig. 3(a). Here the OD was intentionally reduced so that the two minima could be clearly observed. We swept the probe frequency by varying the rf frequency of AOM1 shown in Fig. 2. The sweeping rate was 240 kHz/ μ s, which was slow enough not to cause the transient effect [57]. Asymmetry of the spectrum was caused by the decay of OD during the frequency sweeping. The asymmetry is not a problem, because the value of Ω_c determined in the low- to high-frequency sweeping differed from that in the high- to low-frequency sweeping merely by about 4%. Knowing the value of Ω_c , we then measured the delay time τ_d to determine α as shown in Fig. 3(b), according to $\tau_d = \alpha\Gamma/\Omega_c^2$ [18,58]. A short input pulse with an e^{-1} full width of 3.5 μ s was employed so that the delay time could be determined accurately. Knowing the values of Ω_c and α , we finally measured the peak transmission of the output pulse (T_{\max}) to determine γ as shown in Fig. 3(c), according to $T_{\max} = \exp(-2\alpha\gamma\Gamma/\Omega_c^2)$. A long input pulse with an e^{-1} full width of 35 μ s at the two-photon resonance was employed. Once the values of Ω_c , α , and γ were determined, we further calculated the predictions by numerically solving Eqs. (1)–(3) and compared the short-pulse data with the predictions [similar to Fig. 2(a) in Ref. [44]]. The good agreement between the experimental data and theoretical predictions demonstrates that the values of Ω_c , α , and γ are convincing.

To verify Eq. (12), we controllably introduced fluctuation to the probe frequency via the AOM1 in Fig. 2. In the experiment, the probe pulse was the first-order beam of AOM1. The frequency of the first-order beam can be varied by the modulation voltage of the driver of AOM1. We employed a function generator to produce the voltage of the Gaussian noise. The noise was added to the modulation voltage.

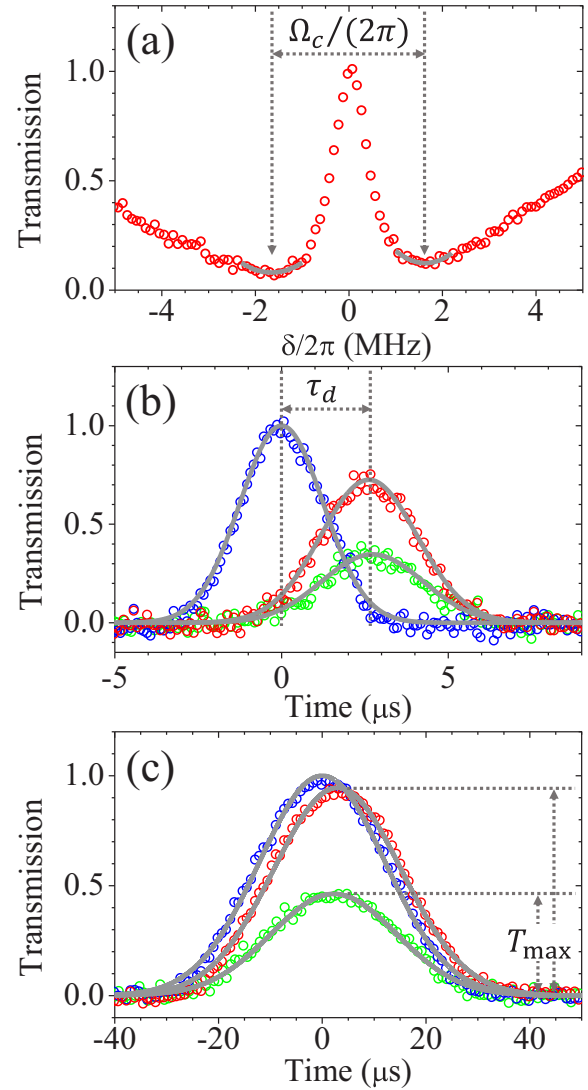


FIG. 3. Determination of experimental parameters in the Λ -EIT study. (a) The EIT spectrum represented by red circles was measured with an intentionally reduced optical depth. The separation distance between two transmission minima determines the coupling Rabi frequency $\Omega_c = 0.54\Gamma$. (b) Slow light data of short probe pulses at $\Omega_c = 0.54\Gamma$. The input pulse is represented by blue circles. The output pulses under the frequency fluctuation $\Gamma_f/2\pi = 0$ and 280 kHz are represented by red and green circles, respectively. Gray lines are the Gaussian best fits to identify peak positions of the pulses. The delay time between the input and output pulses determines the optical depth $\alpha = 29$. (c) Slow light data of long probe pulses at $\Omega_c = 0.54\Gamma$ and $\alpha = 29$. Legends are the same as those in (b). The Gaussian best fits identify peak transmissions of the output pulses, which determine the decoherence rates $\gamma = 2.9 \times 10^{-4}\Gamma$ (red) and $3.9 \times 10^{-3}\Gamma$ (green).

Thus, the first-order beam, i.e., the probe pulse, possessed the Gaussian-distribution frequency fluctuation. Note that the amplitude noise (or power fluctuation) of the probe field, caused by the largest frequency fluctuation in this study, had a standard deviation less than 0.5% of the mean power, which plays a negligible role in the decoherence rate. The center frequency of AOM1 made the two-photon transition resonant.

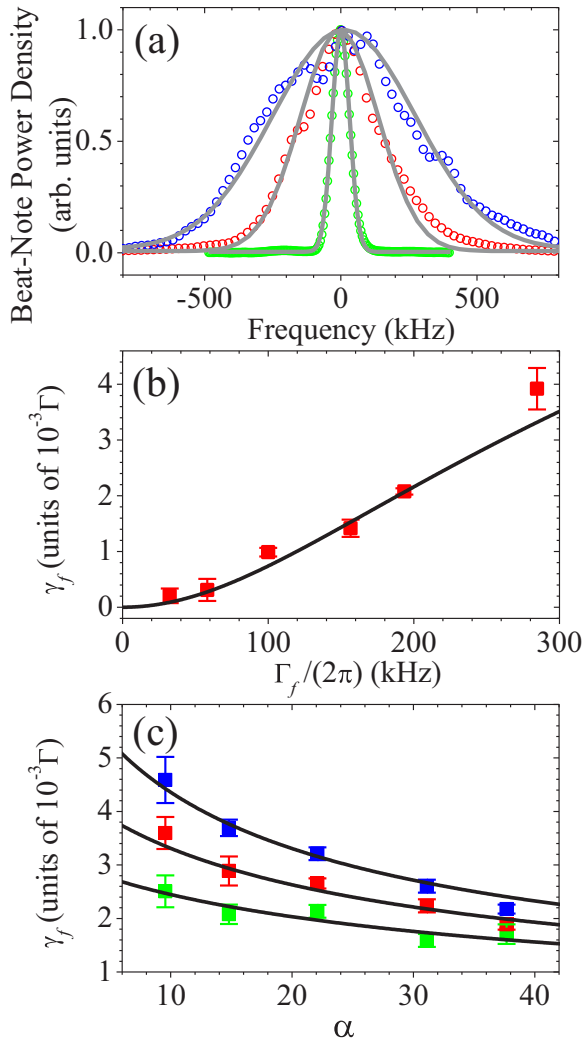


FIG. 4. (a) Representative spectra of beat notes between the first-order and zeroth-order beams of the AOM1 in Fig. 2 under different noise amplitudes Γ_f . Blue, red, and green circles are the spectra and gray lines are the Gaussian best fits. (b) Frequency fluctuation-induced decoherence rate γ_f as a function of Γ_f at $\Omega_c = 0.54\Gamma$ and optical depth $\alpha = 29$. Red squares are the experimental data. (c) Frequency fluctuation-induced decoherence rate γ_f as a function of α at $\Omega_c = 0.44\Gamma$. Blue, red, and green squares are the experimental data measured with $\Gamma_f/2\pi = 220, 180,$ and 150 kHz, respectively. In (b) and (c), black lines are the theoretical predictions according to Eq. (12).

The amplitude of the frequency fluctuation was determined by the beat note between the first-order and zeroth-order beams of AOM1. A photodetector (New Focus 1801) detected the beat note and its output signal was sent to a spectrum analyzer (Agilent EXA N9010A). Figure 4(a) shows representative beat-note spectra measured by the spectrum analyzer. We fitted each spectrum with a Gaussian function. Since the beat note is proportional to the electric field of the first-order beam, Γ_f is equal to the e^{-1} half-width of the best fit divided by $\sqrt{2}$.

The frequency fluctuation-induced decoherence rate γ_f is the difference between the decoherence rates γ with and without the frequency fluctuation. The value of γ was determined by the method depicted in Fig. 3(c). In Fig. 4(b), the red

squares are the experimental data of γ_f as a function of Γ_f , which is the e^{-1} half-width of the Gaussian distribution of the frequency fluctuation. In Fig. 4(c), the green, red, and blue squares represent the experimental data of γ_f as functions of the OD. We subtracted γ_0 [$(4.6 \pm 1.4) \times 10^{-4}\Gamma$] from γ to obtain γ_f in the above measurements. The black lines in Figs. 4(b) and 4(c) represent the theoretical predictions according to Eq. (12), where the calculation parameters of the coupling Rabi frequency, OD, and Γ_f were determined by the methods illustrated in Figs. 3(a), 3(b), and 4(a). The good agreement between the experimental data and the theoretical predictions demonstrates that Eq. (12) is valid.

IV. EXPERIMENT OF RYDBERG-STATE EIT

We now study whether Eq. (11) can quantitatively describe the decoherence rate in the Rydberg-EIT system. The experimental study was carried out with the cold ^{87}Rb atoms trapped by the same MOT [54]. We optically pumped all population to a single Zeeman state of $|5S_{1/2}, F = 2, m_F = 2\rangle$ before any measurement [59]. In the experiment, both the probe and coupling fields were σ_+ polarized. As shown in Fig. 1(b), only the Zeeman states $|1\rangle, |2\rangle,$ and $|3\rangle$ in the levels of $|5S_{1/2}\rangle, |5P_{3/2}\rangle,$ and $|3D_{5/2}\rangle$ were relevant, which can avoid the complexity of multiple EIT subsystems [55,56]. We selected a low principle quantum number of $n = 32$ for the Rydberg state such that the DDI effect can be negligible in this work according to our estimation [60].¹ The wavelengths of the probe and coupling fields were around 780 and 482 nm, respectively. They propagated in opposite directions to minimize the Doppler effect [61]. As the probe and coupling fields interacted with the atoms, their e^{-2} diameters were 300 and 350 μm , respectively. We set the maximum Rabi frequency of the probe field to about 0.034Γ .

The setup of the Rydberg-EIT experiment is depicted in Fig. 5. An ECDL (Toptica DLC DL pro) injection locked or seeded the probe laser. We stabilized the ECDL's frequency by using the Pound-Drever-Hall (PDH) scheme in the saturated-absorption spectrum measured with a hot atomic vapor cell. The bandwidth of the feedback loop for the probe laser in the frequency stabilization system was about 4 MHz. The coupling field was generated by the laser system (Toptica TA-SHG pro). We stabilized the frequency of the coupling laser by using the PDH scheme in the EIT spectrum, in which light beams from the ECDL and the coupling laser interacted with the atomic vapor in another hot vapor cell [47]. The bandwidth of the feedback loop for the coupling laser in the frequency stabilization system was about 50 kHz. We used the AOM3 in Fig. 5 to make the probe frequency seen by the cold atoms resonant to or detuned away from the transition frequency of $|1\rangle \rightarrow |3\rangle$. Since the coupling frequency was kept

¹Following the calculation in Ref. [60], we estimated C_6 of the $32D_{5/2}$ state of Rb atoms to be $-0.66 \text{ GHz } \mu\text{m}^6$. In the experiment, the highest density of Rydberg-state atoms was about $4 \times 10^{13} \text{ m}^{-3}$ according to $n \approx I/\hbar\omega v_g$, where n is the density of Rydberg-state atoms and $I, \hbar\omega,$ and v_g are the intensity, energy per photon, and group velocity of the probe light. Thus, the average frequency shift due to the DDI is less than 8 Hz.

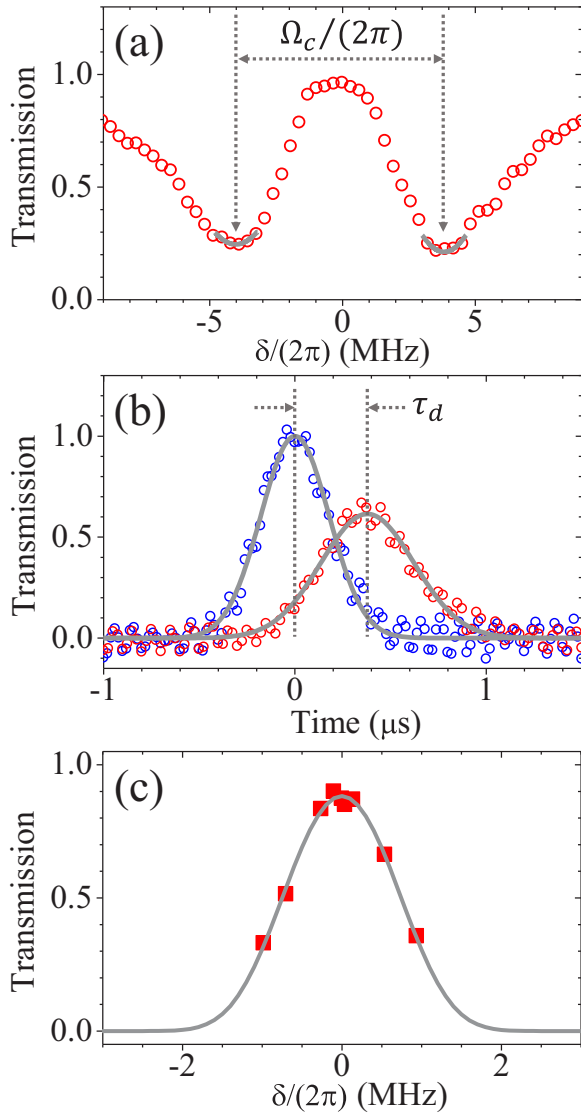


FIG. 7. Determination of experimental parameters in the Rydberg-EIT study. (a) The EIT spectrum represented by red circles was measured with an intentionally reduced optical depth. The separation distance between two transmission minima determines the coupling Rabi frequency $\Omega_c = 1.3\Gamma$. (b) Slow light data of a short probe pulse at $\Omega_c = 1.3\Gamma$. Blue and red circles are the input and output pulses, respectively. Gray lines are the Gaussian best fits to identify peak positions of the pulses. The delay time between the input and output pulses determines the optical depth $\alpha = 25$. (c) Transmission of the output probe pulse as a function of the two-photon detuning at $\Omega_c = 1.3\Gamma$ and $\alpha = 25$. The e^{-1} full width of the input pulse is $7.0 \mu\text{s}$. Red squares are the experimental data. The gray line is the best fit which determines the decoherence rate $\gamma = 4.6 \times 10^{-3}\Gamma$.

the theoretical predictions. Note that for $(\Omega_c^2/\Gamma)/\sqrt{\alpha} \gg 2\Gamma_f$, where $(\Omega_c^2/\Gamma)/\sqrt{\alpha}$ is the e^{-1} full width of EIT window, Eqs. (12) and (11) become

$$\gamma_f \approx \frac{\Gamma}{\Omega_c^2} \Gamma_f^2, \quad (15)$$

$$\gamma \approx \gamma_0 + \frac{\Gamma}{\Omega_c^2} (\Gamma_D^2 + \Gamma_f^2). \quad (16)$$

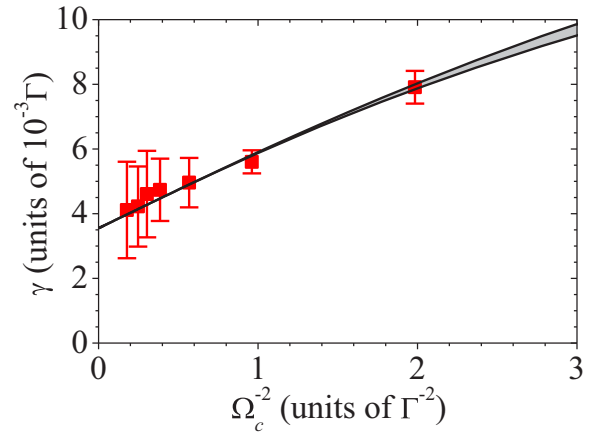


FIG. 8. Decoherence rate γ in the Rydberg-EIT system as a function of Ω_c^{-2} . Red squares are the averages of data taken at different optical depths $\alpha = 15$ –26. Two black lines, corresponding to $\alpha = 15$ (upper) and 26 (lower), are the theoretical predictions of Eq. (11). The predictions were calculated with $\gamma_0 = 3.6 \times 10^{-3}\Gamma$ or $2\pi \times 22$ kHz, $\Gamma_D = 2\pi \times 200$ kHz, and $\Gamma_f = 2\pi \times 210$ kHz (see the text for how to determine these values).

Hence, γ is linearly proportional to $1/\Omega_c^2$ and becomes independent of α at large values of Ω_c , as shown in Fig. 8. The good agreement between the data and predictions shows that the theoretical model or Eq. (11) in this work describes the decoherence processes in the Rydberg-EIT system very well.

After the amount of frequency fluctuation due to the laser frequency stabilization system was confirmed in Fig. 8, we further studied the decoherence rate γ as a function of the frequency fluctuation Γ_f , as shown in Fig. 9. The additional frequency fluctuation was introduced via the AOM3 in Fig. 5 in the same way as we described in Sec. III. The amplitude noise (or power fluctuation) of the probe field, caused by the largest frequency fluctuation introduced to the AOM3, had a standard deviation of about 0.4% of the mean power,

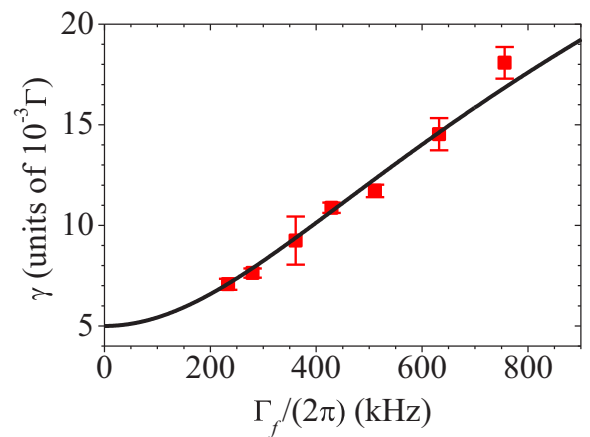


FIG. 9. Decoherence rate γ in the Rydberg-EIT system as a function of frequency fluctuation Γ_f . In the measurement, $\Omega_c = 0.83\Gamma$ and optical depth $\alpha = 18$. Red squares are the experimental data and the black line is the theoretical prediction according to Eq. (11).

which plays a negligible role in the decoherence rate. Now the value of Γ_f is equal to $\sqrt{\Gamma_{f,\text{laser}}^2 + \Gamma_{f,\text{AOM}}^2}$, where $\Gamma_{f,\text{laser}}$ is the frequency fluctuation due to the stabilization system and $\Gamma_{f,\text{AOM}}$ is the frequency fluctuation due to the AOM3. We employed a Gaussian input pulse with an e^{-1} full width of $7.0 \mu\text{s}$ in the measurement and determined the value of γ by the transmission of the output pulse. In Fig. 9, the consistency between the experimental data and theoretical prediction is satisfactory.

Finally, one might worry that the separation distance between two transmission minima $\Delta\omega_{\text{AT}}$ in Fig. 7(a) and the delay time τ_d in Fig. 7(b) can be influenced by the effects of frequency fluctuation and atomic motion. The two effects, i.e., Γ_f and Γ_D , were switched off or are negligible in Figs. 3(a) and 3(b), but must be present in Figs. 7(a) and 7(b). Using Eqs. (4), (7), and (9), we derive the values of $\Delta\omega_{\text{AT}}$ and τ_d in the presence of Γ_f and Γ_D . It can be shown that

$$\Delta\omega_{\text{AT}} = \Omega_c \left[1 + \frac{3(\Gamma_f^2 + \Gamma_D^2)}{\Omega_c^2} \right], \quad (17)$$

$$\tau_d = \frac{\alpha\Gamma}{\Omega_c^2} \left[1 + \frac{6(\Gamma_f^2 + \Gamma_D^2)(\Omega_c^2 - \Gamma^2)}{\Omega_c^4} \right]. \quad (18)$$

In our system, $\Gamma_f = 2\pi \times 210 \text{ kHz}$ and $\Gamma_D = 2\pi \times 200 \text{ kHz}$. The minimum value of Ω_c in this study was 0.71Γ or $2\pi \times 4.3 \text{ MHz}$. Therefore, the $\Delta\omega_{\text{AT}} = \Omega_c$ and $\tau_d = \alpha\Gamma/\Omega_c^2$ used in Figs. 7(a) and 7(b) are good approximations.

V. CONCLUSION

In this work we systematically studied the effect of laser frequency fluctuation on the decoherence rate of the Λ -type and Rydberg-state EIT systems. The laser frequency fluctuation randomly introduces a two-photon detuning to the system, resulting in attenuation of the probe field. The attenuation is equivalent to an increment of the decoherence rate. Using the steady-state solution of the optical Bloch equation and the Maxwell-Schrödinger equation, we derived the formula in Eq. (12) to describe the frequency-fluctuation-induced decoherence rate γ_f . The formula for γ_f was tested in the Λ -EIT

system with laser-cooled ^{87}Rb atoms. The experimental data of γ_f are in good agreement with the theoretical predictions of Eq. (12).

We further studied the decoherence processes in the Rydberg-EIT system, in which moving atoms induce non-negligible two-photon detunings due to the Doppler shift. We considered the distribution of the Doppler shift among the atoms and obtained the formula in Eq. (13) to describe the Doppler shift-induced decoherence rate γ_D . The total effective decoherence rate γ shown in Eq. (11) consists of three parts γ_f , γ_D , and γ_0 , with γ_0 an intrinsic decoherence rate in the system. The experimental study of γ was carried out with cold atoms of $350 \mu\text{K}$. We utilized the Rydberg state of $|32D_{5/2}\rangle$, in which the dipole-dipole interaction can be neglected. A rather low value of γ of $2\pi \times 48 \text{ kHz}$ was achieved at a moderate coupling Rabi frequency Ω_c of $2\pi \times 4.3 \text{ MHz}$. The experimental data of γ are consistent with the theoretical predictions.

According to Eqs. (11)–(13), larger values of Ω_c make smaller γ . Furthermore, as the EIT linewidth is much greater than the amplitude of the frequency fluctuation, γ is linearly proportional to $1/\Omega_c^2$ and asymptotically approaches γ_0 . In our Rydberg-EIT system, γ_0 is approximately $2\pi \times 22 \text{ kHz}$, which comes from the natural linewidth of the Rydberg state, the Lorentzian-type laser linewidths of the probe and coupling fields, and other decoherence processes. The results of our work are useful for the estimation of outcomes or decoherence rates of Rydberg-EIT experiments and provide a better understanding of the Rydberg-EIT effect.

ACKNOWLEDGMENTS

This work was supported by the Ministry of Science and Technology of Taiwan, under Grants No. 105-2923-M-007-002-MY3, No. 106-2119-M-007-003, and No. 107-2745-M-007-001, and the project TAP No. LLT-2/2016 of the Research Council of Lithuania. J.R. and G.J. also acknowledge support from the National Center for Theoretical Sciences, Taiwan. The authors thank Dr. Ming-Shien Chang for lending us the laser system of Toptica TA-SHG pro.

-
- [1] L. Isenhower, E. Urban, X. L. Zhang, A. T. Gill, T. Henage, T. A. Johnson, T. G. Walker, and M. Saffman, *Phys. Rev. Lett.* **104**, 010503 (2010).
 - [2] T. Wilk, A. Gaëtan, C. Evellin, J. Wolters, Y. Miroshnychenko, P. Grangier, and A. Browaeys, *Phys. Rev. Lett.* **104**, 010502 (2010).
 - [3] H. Levine, A. Keesling, A. Omran, H. Bernien, S. Schwartz, A. S. Zibrov, M. Endres, M. Greiner, V. Vuletić, and M. D. Lukin, *Phys. Rev. Lett.* **121**, 123603 (2018).
 - [4] M. Saffman and T. G. Walker, *Phys. Rev. A* **66**, 065403 (2002).
 - [5] L. Li and A. Kuzmich, *Nat. Commun.* **7**, 13618 (2016).
 - [6] H. Weimer, M. Müller, I. Lesanovsky, P. Zoller, and H. P. Büchler, *Nat. Phys.* **6**, 382 (2010).
 - [7] H. Kim, Y. J. Park, K. Kim, H.-S. Sim, and J. Ahn, *Phys. Rev. Lett.* **120**, 180502 (2018).
 - [8] D. Tong, S. M. Farooqi, J. Stanojevic, S. Krishnan, Y. P. Zhang, R. Côté, E. E. Eyler, and P. L. Gould, *Phys. Rev. Lett.* **93**, 063001 (2004).
 - [9] K. Singer, M. Reetz-Lamour, T. Amthor, L. G. Marcassa, and M. Weidemüller, *Phys. Rev. Lett.* **93**, 163001 (2004).
 - [10] R. Heidemann, U. Raitzsch, V. Bendkowsky, B. Butscher, R. Löw, L. Santos, and T. Pfau, *Phys. Rev. Lett.* **99**, 163601 (2007).
 - [11] A. Gaëtan, Y. Miroshnychenko, T. Wilk, A. Chotia, M. Viteau, D. Comparat, P. Pillet, A. Browaeys, and P. Grangier, *Nat. Phys.* **5**, 115 (2009).
 - [12] D. Comparat and P. Pillet, *J. Opt. Soc. Am. B* **27**, A208 (2010).
 - [13] A. V. Gorshkov, J. Otterbach, M. Fleischhauer, T. Pohl, and M. D. Lukin, *Phys. Rev. Lett.* **107**, 133602 (2011).
 - [14] Y. O. Dudin and A. Kuzmich, *Science* **336**, 887 (2012).

- [15] L. Béguin, A. Vernier, R. Chicireanu, T. Lahaye, and A. Browaeys, *Phys. Rev. Lett.* **110**, 263201 (2013).
- [16] C. Tresp, C. Zimmer, I. Mirgorodskiy, H. Gorniaczyk, A. Paris-Mandoki, and S. Hofferberth, *Phys. Rev. Lett.* **117**, 223001 (2016).
- [17] F. Ripka, H. Kübler, R. Löw, and T. Pfau, *Science* **362**, 446 (2018).
- [18] M. Fleischhauer, A. Imamoglu, and J. P. Marangos, *Rev. Mod. Phys.* **77**, 633 (2005).
- [19] C.-K. Chiu, Y.-H. Chen, Y.-C. Chen, I. A. Yu, Y.-C. Chen, and Y.-F. Chen, *Phys. Rev. A* **89**, 023839 (2014).
- [20] Z.-Y. Liu, Y.-H. Chen, Y.-C. Chen, H.-Y. Lo, P.-J. Tsai, I. A. Yu, Y.-C. Chen, and Y.-F. Chen, *Phys. Rev. Lett.* **117**, 203601 (2016).
- [21] J. D. Pritchard, D. Maxwell, A. Gauguier, K. J. Weatherill, M. P. A. Jones, and C. S. Adams, *Phys. Rev. Lett.* **105**, 193603 (2010).
- [22] S. Sevinçli, N. Henkel, C. Ates, and T. Pohl, *Phys. Rev. Lett.* **107**, 153001 (2011).
- [23] D. Petrosyan, J. Otterbach, and M. Fleischhauer, *Phys. Rev. Lett.* **107**, 213601 (2011).
- [24] S. Sevinçli, C. Ates, T. Pohl, H. Schempp, C. S. Hofmann, G. Günter, T. Amthor, M. Weidemüller, J. D. Pritchard, D. Maxwell, A. Gauguier, K. J. Weatherill, M. P. A. Jones, and C. S. Adams, *J. Phys. B* **44**, 184018 (2011).
- [25] T. Peyronel, O. Firstenberg, Q.-Y. Liang, S. Hofferberth, A. V. Gorshkov, T. Pohl, M. D. Lukin, and V. Vuletić, *Nature (London)* **488**, 57 (2012).
- [26] B. He, A. V. Sharypov, J. Sheng, C. Simon, and M. Xiao, *Phys. Rev. Lett.* **112**, 133606 (2014).
- [27] O. Firstenberg, C. S. Adams, and S. Hofferberth, *J. Phys. B* **49**, 152003 (2016).
- [28] D. Tiarks, S. Schmidt-Eberle, T. Stolz, G. Rempe, and S. Dürr, *Nat. Phys.* **15**, 124 (2018).
- [29] Y.-F. Chen, C.-Y. Wang, S.-H. Wang, and I. A. Yu, *Phys. Rev. Lett.* **96**, 043603 (2006).
- [30] Y.-W. Lin, W.-T. Liao, T. Peters, H.-C. Chou, J.-S. Wang, H.-W. Cho, P.-C. Kuan, and I. A. Yu, *Phys. Rev. Lett.* **102**, 213601 (2009).
- [31] K. M. Beck, M. Hosseini, Y. Duan, and V. Vuletić, *Proc. Natl. Acad. Sci. USA* **113**, 9740 (2016).
- [32] E. Distante, A. Padrón-Brito, M. Cristiani, D. Paredes-Barato, and H. de Riedmatten, *Phys. Rev. Lett.* **117**, 113001 (2016).
- [33] J. Ruseckas, I. A. Yu, and G. Juzeliūnas, *Phys. Rev. A* **95**, 023807 (2017).
- [34] S. Baur, D. Tiarks, G. Rempe, and S. Dürr, *Phys. Rev. Lett.* **112**, 073901 (2014).
- [35] D. Tiarks, S. Schmidt, G. Rempe, and S. Dürr, *Sci. Adv.* **2**, e1600036 (2016).
- [36] C. R. Murray, I. Mirgorodskiy, C. Tresp, C. Braun, A. Paris-Mandoki, A. V. Gorshkov, S. Hofferberth, and T. Pohl, *Phys. Rev. Lett.* **120**, 113601 (2018).
- [37] M. Fleischhauer and M. D. Lukin, *Phys. Rev. Lett.* **84**, 5094 (2000).
- [38] G. Juzeliūnas and H. J. Carmichael, *Phys. Rev. A* **65**, 021601(R) (2002).
- [39] K. J. Weatherill, J. D. Pritchard, R. P. Abel, M. G. Bason, A. K. Mohapatra, and C. S. Adams, *J. Phys. B* **41**, 201002 (2008).
- [40] S. de Léséleuc, D. Barredo, V. Lienhard, A. Browaeys, and T. Lahaye, *Phys. Rev. A* **97**, 053803 (2018).
- [41] R. Legaie, C. J. Picken, and J. D. Pritchard, *J. Opt. Soc. Am. B* **35**, 892 (2018).
- [42] Y. Zeng, K.-P. Wang, Y.-Y. Liu, X.-D. He, M. Liu, P. Xu, J. Wang, and M.-S. Zhan, *J. Opt. Soc. Am. B* **35**, 454 (2018).
- [43] C. J. Picken, R. Legaie, K. McDonnell, and J. D. Pritchard, *Quantum Sci. Technol.* **4**, 015011 (2019).
- [44] Y.-H. Chen, M.-J. Lee, I.-C. Wang, S. Du, Y.-F. Chen, Y.-C. Chen, and I. A. Yu, *Phys. Rev. Lett.* **110**, 083601 (2013).
- [45] J. de Hond, N. Cisternas, G. Lohead, and N. J. van Druten, *Appl. Opt.* **56**, 5436 (2017).
- [46] M. Mack, F. Karlewski, H. Hattermann, S. Höckh, F. Jessen, D. Cano, and J. Fortágh, *Phys. Rev. A* **83**, 052515 (2011).
- [47] R. P. Abel, A. K. Mohapatra, M. G. Bason, J. D. Pritchard, K. J. Weatherill, U. Raitzsch, and C. S. Adams, *Appl. Phys. Lett.* **94**, 071107 (2009).
- [48] J. Gea-Banacloche, Y.-Q. Li, S.-Z. Jin, and M. Xiao, *Phys. Rev. A* **51**, 576 (1995).
- [49] Y.-Q. Li, S.-Z. Jin, and M. Xiao, *Phys. Rev. A* **51**, R1754 (1995).
- [50] B. Lü, W. H. Burkett, and M. Xiao, *Phys. Rev. A* **56**, 976 (1997).
- [51] J. Han, T. Vogt, and W. Li, *Phys. Rev. A* **94**, 043806 (2016).
- [52] S.-C. Gou, S.-W. Su, and I. A. Yu, *Phys. Rev. A* **96**, 047801 (2017).
- [53] S.-W. Su, Y.-H. Chen, S.-C. Gou, T.-L. Horng, and I. A. Yu, *Phys. Rev. A* **83**, 013827 (2011).
- [54] Y.-W. Lin, H.-C. Chou, P. P. Dwivedi, Y.-C. Chen, and I. A. Yu, *Opt. Express* **16**, 3753 (2008).
- [55] Y.-F. Chen, P.-C. Kuan, S.-H. Wang, C.-Y. Wang, and I. A. Yu, *Opt. Lett.* **31**, 3511 (2006).
- [56] T. Peters, Y.-H. Chen, J.-S. Wang, Y.-W. Lin, and I. A. Yu, *Opt. Express* **17**, 6665 (2009).
- [57] Y.-F. Chen, G.-C. Pan, and I. A. Yu, *J. Opt. Soc. Am. B* **21**, 1647 (2004).
- [58] Y.-F. Chen, Y.-M. Kao, W.-H. Lin, and I. A. Yu, *Phys. Rev. A* **74**, 063807 (2006).
- [59] M.-J. Lee, J. Ruseckas, C.-Y. Lee, V. Kudriašov, K.-F. Chang, H.-W. Cho, G. Juzeliūnas, and I. A. Yu, *Nat. Commun.* **5**, 5542 (2014).
- [60] T. G. Walker and M. Saffman, *Phys. Rev. A* **77**, 032723 (2008).
- [61] M. Xiao, Y.-Q. Li, S.-Z. Jin, and J. Gea-Banacloche, *Phys. Rev. Lett.* **74**, 666 (1995).
- [62] B. Zhao, Y.-A. Chen, X.-H. Bao, T. Strassel, C.-S. Chuu, X.-M. Jin, J. Schmiedmayer, Z.-S. Yuan, S. Chen, and J.-W. Pan, *Nat. Phys.* **5**, 95 (2009).
- [63] S.-W. Su, Y.-H. Chen, S.-C. Gou, and I. A. Yu, *J. Phys. B* **44**, 165504 (2011).